

On the role of the MJO in exciting El Niño

Geert Jan van Oldenborgh

KNMI, P.O. Box 210, 3730 AE De Bilt, the Netherlands
oldenborgh@knmi.nl

ABSTRACT

The role of intraseasonal variability in the tropics in exciting El Niño is investigated. The most important component is the zonal wind in the equatorial wave guide, 5°S–5°N, in the west and central Pacific, 130°E–160°W. This is correlated to the MJO, but there are components that are independent. We subtract the influence of ENSO on the indices of intraseasonal variability as well as from the evolution of the Niño3 index itself. Statistically, there is a strong lag correlation of zonal wind with deviations of the standard ENSO cycle four months later. The connection with the MJO is similar but weaker. The MJO only influences El Niño through its mean, the intraseasonal variability does not seem to play a role. In contrast, the correlation with the monthly mean zonal wind is roughly equal to the correlation with its monthly variability. The first effect can be understood as linear integration of high-frequency variability into lower-frequency variations by the ocean, the effect of the variability must be due to non-linear interactions. Finally, the mean zonal wind stress is correlated to central Pacific SST not in phase with eastern Pacific SST, so that models that represent the central Pacific well can be expected to predict the onset of El Niño better than models that do not include warm pool physics correctly.

1 Ideas

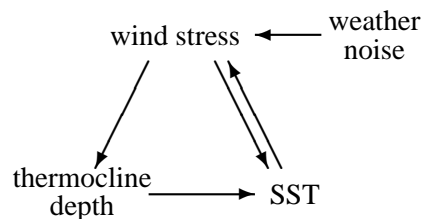


Figure 1: A schematic picture of the ENSO cycle

A schematic picture of the ENSO cycle is given in Fig. 1. Wind stress anomalies on the equator in the western and central Pacific cause thermocline depth anomalies; wave dynamics transport these to the east where they are advected up as SST anomalies. These in turn affect the wind. Wind anomalies also influence SST directly, especially in the western and central Pacific.

2 Case study: 1997/98

The onset of the very strong 1997/98 El Niño was preceded by very strong westerly wind events in the western Pacific (e.g. [McPhaden, 1999](#)). These in turn coincided with strong Madden-Julian oscillations. Although a causal relationship seems obvious, modelling studies diverge on its influence. Among the many studies, [van Oldenborgh \(2000\)](#) concluded that the steep onset was mostly due to the westerly wind events in February,

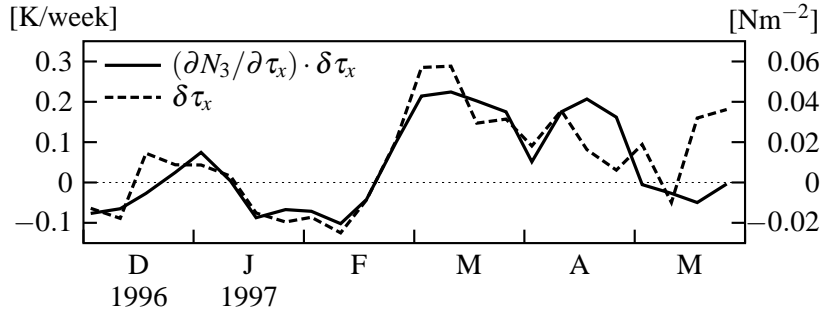


Figure 2: The influence of zonal wind stress on the Niño3 index on Jun 1, 1997 (solid line) and the zonal wind stress in the area 5°S – 5°N , 130°E – 160°E (dashed line).

March and April 1997, and hence unpredictable. However, the actual forecast from the December 1, 1996 analysis of the ECMWF seasonal forecast System-1, based on essentially the same ocean model, were in fact very good, although they did not include these wind events. This discrepancy will be investigated here.

The spatial and temporal patterns influencing the strength of El Niño can be studied using an adjoint model (van Oldenborgh et al., 1999; Galanti and Tziperman, 2002). Only the adjoint ocean model is considered, which means that coupled interactions on time scales shorter than the run are neglected. During the onset phase this is a reasonable assumption for the eastern Pacific, but it is not so good in the central Pacific (see also Boulanger, these proceedings). Using this adjoint, deviations of the Niño3 index on a given date from climatology can be computed as

$$\Delta N_3 = \int_0^T dt \frac{\partial N_3}{\partial \tau_x(t)} \cdot \Delta \tau_x(t) + \frac{\partial N_3}{\partial T_0} \cdot \Delta T_0 + \text{smaller terms} \quad (1)$$

where the partial derivatives are computed by the adjoint model, $\Delta \tau_x(t)$ is the anomalous zonal wind stress and ΔT_0 the anomalous 3D ocean temperature field at the start of the experiment. The dots indicate integration over the surface and ocean volume respectively.

Specifically, for the 6-month forecast starting Dec 1, 1996 the influence of zonal wind stress on the Niño3 index at Jun 1, 1997 is shown in Figure 2. The zonal wind stress term explained about half of the rise of the Niño3 index, the other half was due to the initial state temperature: a deeper thermocline in the west Pacific. As can be seen in Fig. 2, the time evolution of the contribution of the zonal wind stress parallels the zonal wind stress in the equatorial wave guide, so the sensitivity is quite constant in this area. The spatial structure is illustrated in Fig. 3, which shows the week of the large westerly wind event around March 11, 1997. The spatial sensitivity is also quite constant in the area of interest (the large sensitivities in the eastern Pacific are due to model error caused by a target function with sharp corners, see Galanti and Tziperman (2002) for a better function).

3 Statistics

The connections between the MJO, westerly wind in the equatorial wave guide and ENSO are investigated further using statistical methods over the last 15–25 years. For the MJO we use the 5-daily MJO01 index of the CPC minus MJO06 (1978–2003, Xue, 2003), the westerly wind has been measured by the TAO array (~1990–2002, McPhaden et al., 1998) and the Niño3 index is derived from the weekly Reynolds OIv2 analyses (1981–2003, Reynolds et al., 2002). These are plotted in Fig. 4 for the years 1996–1998. One immediately sees

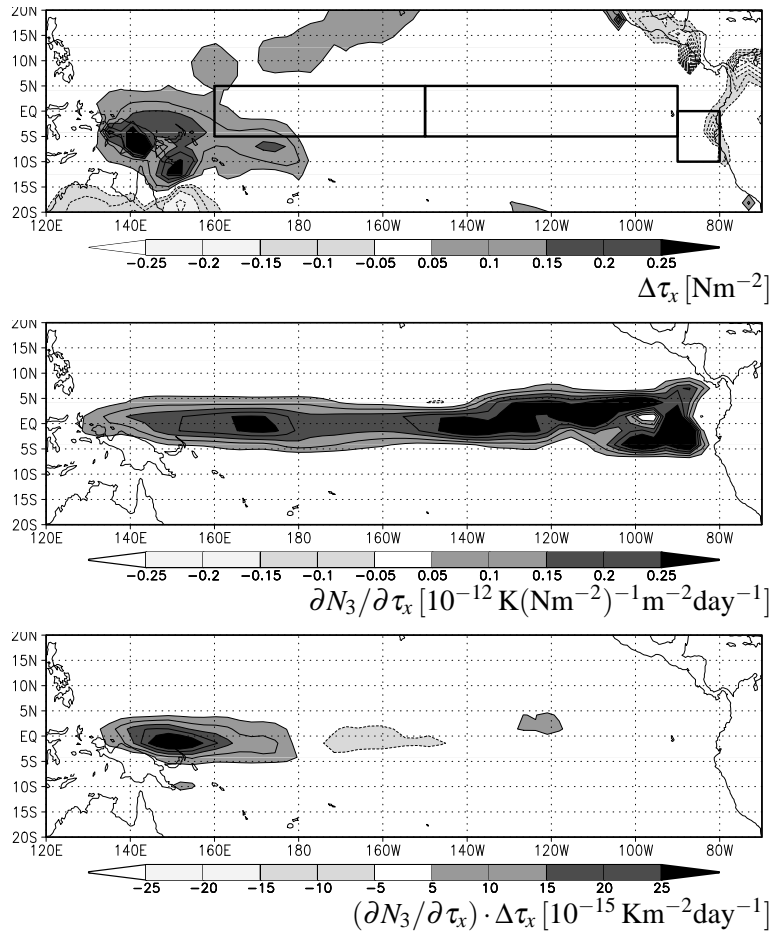


Figure 3: The anomalous wind stress in the week centered on March 11, 1997 (top), the sensitivity of the Niño3 index on Jun 1, 1997 to this zonal wind stress (middle), and the product of the two, which describes the influence on the Niño3 index (bottom, cf. Eq. 1).

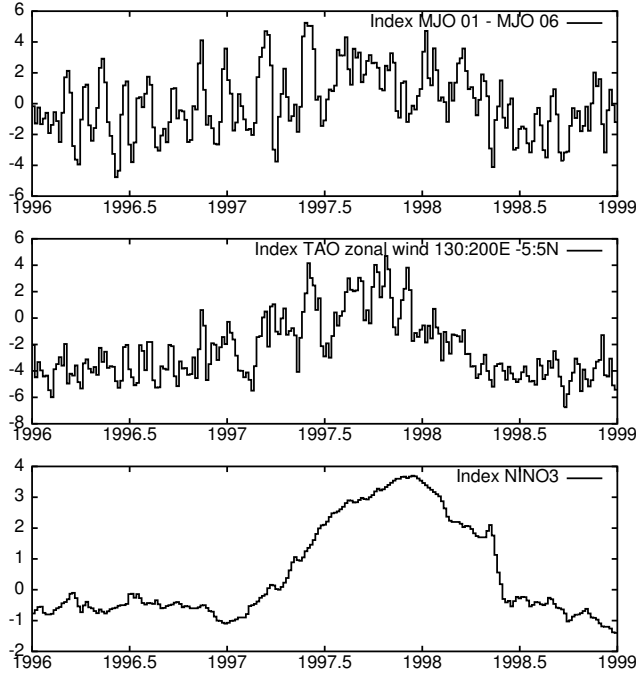


Figure 4: Time series of indices of the MJO (top), 4m wind in the area 5°S – 5°N , 130°E – 160°W and ENSO (Niño3, bottom).

that both the MJO index and the westerly wind stress have a component that is part of the ENSO cycle. This component also shows up in lag-correlations between these three indices (Fig. 5) as a positive correlation that varies slowly over the course of the two years shown.

The ENSO cycle component is removed by subtracting linear regressions with the Niño3 index:

$$N'_{3,l}(t) = N_3 - \alpha(m, l)N_3(t - l) \quad (2)$$

at lag $l = 4$ months, and the MJO and 4m zonal wind indices with the simultaneous influence of Niño3 subtracted

$$\text{MJO}'(t) = \text{MJO}(t) - \beta(m)N_3(t) \quad (3)$$

$$u'(t) = u(t) - \gamma(m)N_3(t) \quad (4)$$

In the case of the Niño3 index this removes the (scaled) persistence, in the case of the MJO and zonal wind stress indices it removes the predictable component related to the ENSO cycle (Fig. 1) itself.

The indices without ENSO cycle show clear causal relationships. The MJO' has a simultaneous correlation with the westerly wind index u' of $r = 0.48$ for the 5-daily data, so it only explains one quarter of the variance. The lag correlation of the u' with N'_3 has exactly the expected lag structure (Fig. 6, left): ENSO leading does not give any effect (this has been subtracted), but westerly wind activity is followed by a rise in the N'_3 index a few months later. The lag correlation plot with the MJO' shows the same structure, but much weaker.

To investigate the scale interactions the lag correlations have also been computed for the monthly mean and the monthly standard deviation of the indices. The MJO monthly mean has more predictive power than the 5-day average, but the variability has no effect at all on ENSO. The term 'Madden-Julian Oscillations' is usually used

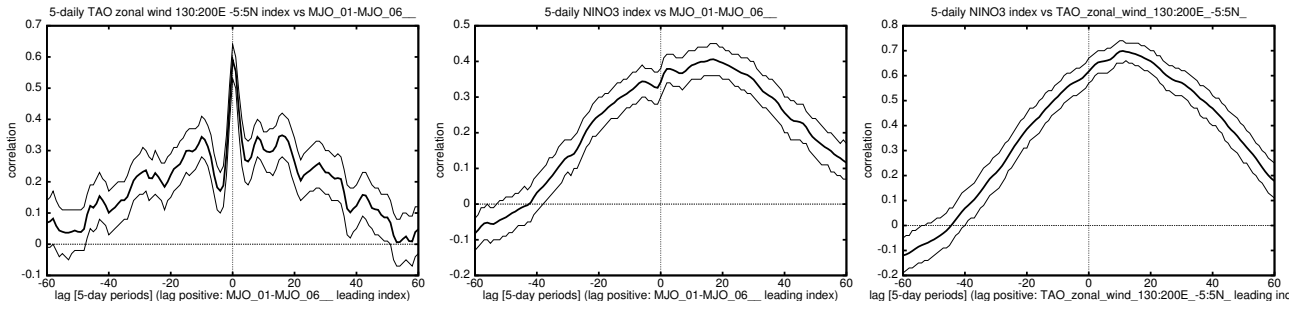


Figure 5: Lag correlations of the 5-daily equatorial zonal surface wind versus MJO indices (left), Niño3 versus the MJO index (middle) and the Niño3 index versus zonal wind stress (right). (The 95% confidence interval (thin lines) does not take into account the non-zero auto-correlations and are therefore too narrow.)

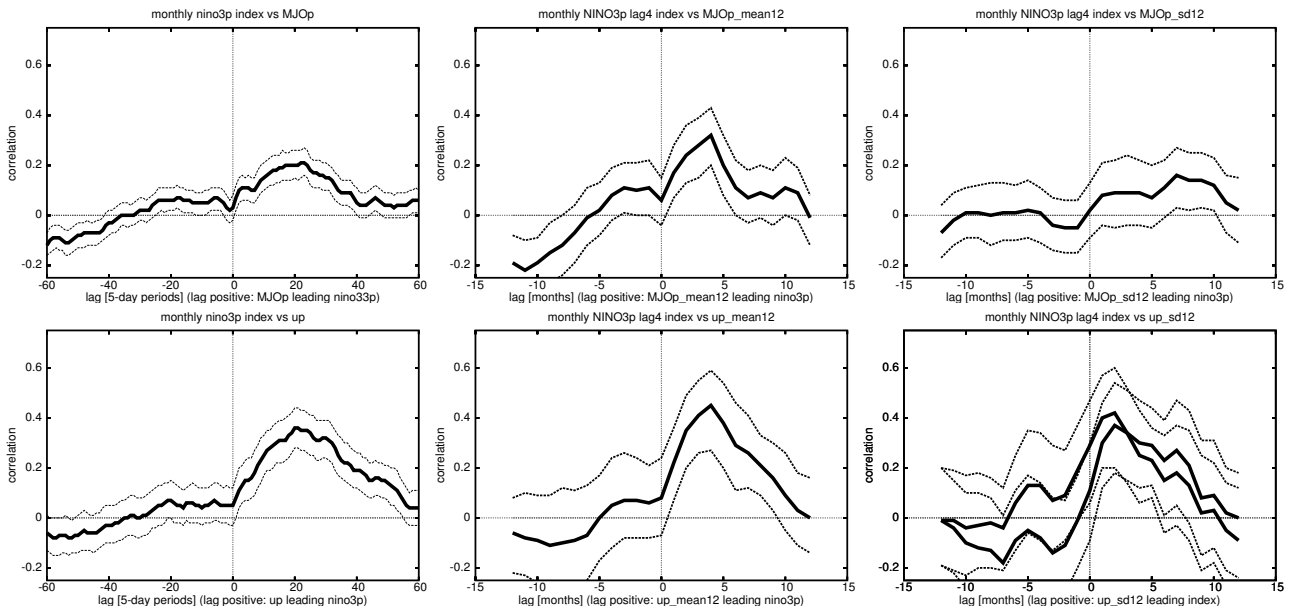


Figure 6: Lag correlations of N_3' with MJO' (top) and u' (bottom). Left: 5-daily data; center: monthly mean and right: monthly standard deviation; the second (lower) curve for the zonal wind stress has the ENSO cycle again subtracted. (The 95% CL error bars for the daily data underestimate the true uncertainty due to autocorrelations that have not been taken into account.)

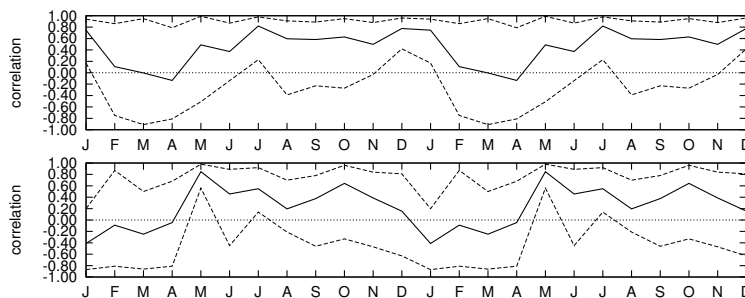


Figure 7: The correlation between zonal mean westerly wind monthly mean (top) and standard deviation (bottom) with the Niño3 four months later. The months show the time the Niño3 index was perturbed. All quantities have the linear regression with Niño3 removed. The dashed lines indicate the 95% confidence interval.

for the variability with a period of 40–50 days (Madden and Julian, 1971). This variability shows up strongly in the monthly standard deviation. The lack of lag correlation of the monthly standard deviation with Niño3 indicates that MJO oscillations are not very relevant to ENSO variability and will no longer be considered.

The zonal wind stress has more predictive power. This was also expected on the basis of sensitivity studies such as discussed for the 1997/98 event. The lag correlations are about the same for the mean and the variability, with correlations of $r = 0.4 \dots 0.5$ for monthly means, about 0.6 for 3-month means. The standard deviation has a small component that is related to the ENSO cycle ($r = 0.28^{+18}_{-20}$ with the Niño3 index, 95% confidence interval). This may be due to a larger warm pool during El Niño that allows the westerly wind events to extend further to the east, increasing variability. However, subtracting this effect makes very little difference (lower curve in Fig. 6, lower right). The standard deviation is also related to the mean, as westerly wind event increase both. However, this effect is quite small, $r = 0.26^{+15}_{-17}$.

Linear wave dynamics shows that the lagged correlation of N'_3 and mean zonal wind is due to a causal relationship. The ocean integrates the high frequency wind stress variations into a low frequency signal. This signal is very similar to the Warm Water Volume of Kessler (2002) and the available potential energy of Fedorov et al. (2003) and is known to precede El Niño events. In fact a linear ENSO model driven by stochastic noise with amplitude and time structure derived from observations simulates ENSO quite well, see Burgers and van Oldenborgh (2003). The signal speed is slower than the speed of a free Kelvin wave, with maximum effect of SST peaking about at around four months after the wind anomaly. The reasons for this are discussed e.g. in the review of Neelin et al. (1998).

The interpretation of the lagged correlation with zonal wind speed variability as a causal effect is also supported by theory of non-linear interactions and GCM simulations, see for instance the article by Boulanger *et al* in these proceedings. The lagged relationship peaks at shorter time scales of about two months.

Finally, it should be noted that the effects shown have a strong dependence on the seasonal cycle. In fact, the varying sensitivity to wind stress is one of the main reasons for the seasonal cycle (Galanti and Tziperman, 2000). Looking at a lag of four months, one sees that the correlation to the monthly mean is strong from July through January ($r = 0.64^{+14}_{-22}$, 95% CL, see Fig. 7, top). This corresponds to westerly wind in March to September. The correlation is virtually zero the rest of the year ($r = 0.20^{+30}_{-32}$). For the standard deviation the active season is shifted slightly to May–November Niño3 ($r = 0.42^{+18}_{-19}$, Fig. 7, bottom), corresponding to westerly wind variability in January to July, when SST is highest. Again there is very little correlation in the other months ($r = -0.13^{+26}_{-27}$).

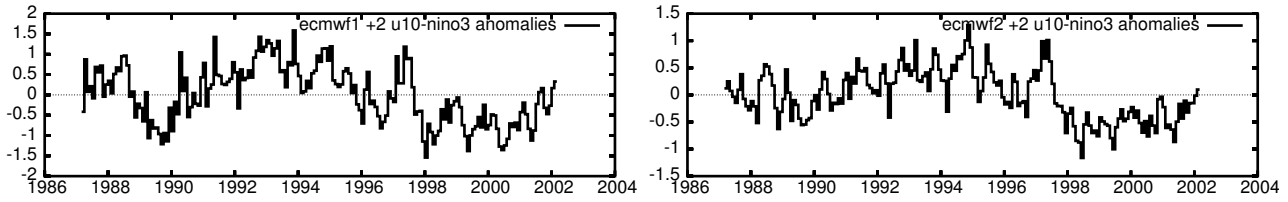


Figure 8: The 2-month forecast mean zonal wind stress anomalies (minus the regression against model Niño3) in System-1 (left) and System-2 (right).

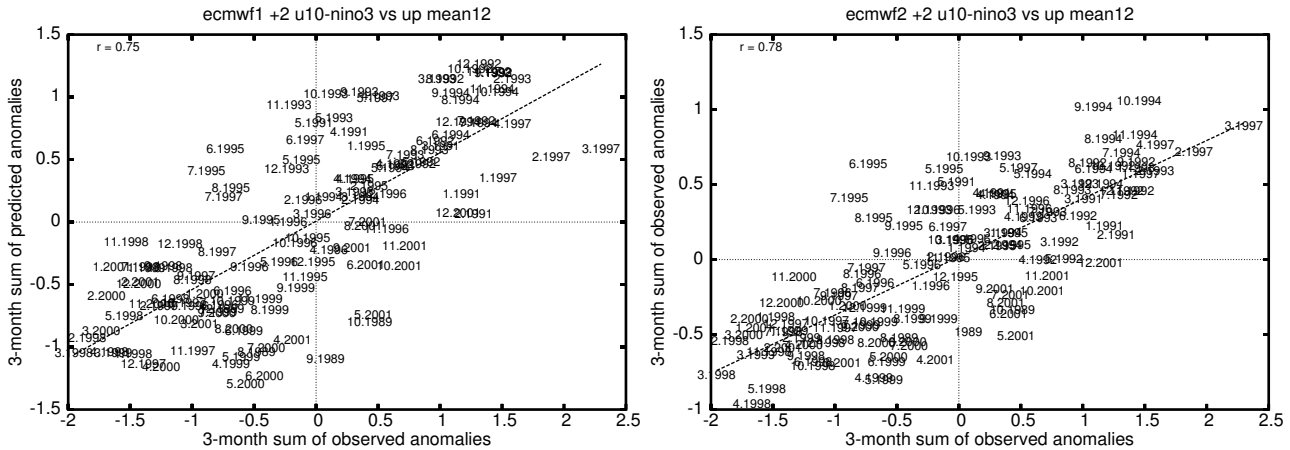


Figure 9: The 3-month average +2 forecast mean zonal wind stress anomalies (minus the regression against model Niño3) of System-1 (left) and System-2 (right) verified against TAO observations.

The sensitivities probably also depend strongly on the ENSO cycle, but this has not been investigated here.

4 Predictability

The monthly mean zonal wind stress with ENSO cycle subtracted is forecast very well by the ECMWF seasonal models. The +2-month ensemble mean forecasts of the old System-1 that made real-time forecasts in 1996/97 and the newer System-2 hindcasts are shown in Fig. 8. As usual, the System-2 forecasts are damped with respect to System-1, but both in the long-term trends and in shorter variations they match well. They also verify well against the TAO observations (Fig. 9), with anomaly correlations of 0.75 and 0.78 for 3-month means.

The zonal wind stress minus the regression with Niño3 was associated with the SST patterns in the month before analysis time shown in Fig. 10. These patterns give rise to the predictability of the mean zonal wind stress in the equatorial wave guide, apart from the ENSO cycle. They very similar to the SST pattern associated with the Niño4 variability with Niño3 subtracted over the same period, shown also in the figure.

This can also be seen from the direct comparisons of the observed wind stress with the Niño4 index, Fig. 11, both again with the ENSO cycle as parametrized by the Niño3 index subtracted. The independent role of the central Pacific, with its longer persistence, in the ENSO cycle has also been emphasized in Burgers and van Oldenborgh (2003).

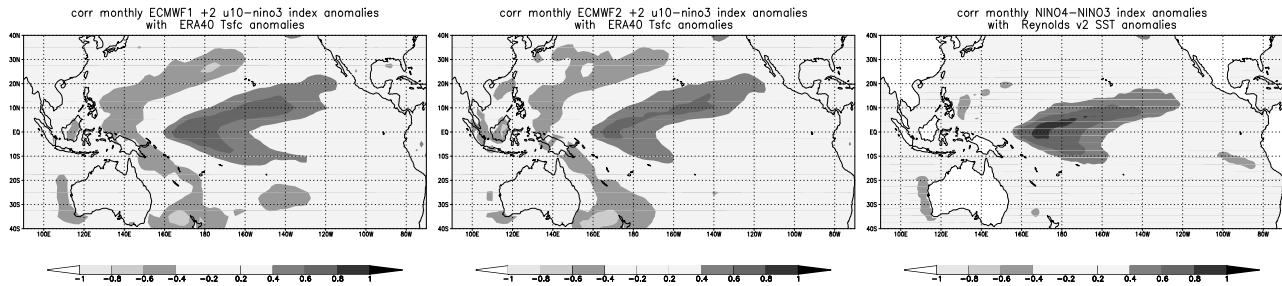


Figure 10: The SST pattern in the month preceding the analysis time correlated with the 3-month average +2 forecast mean zonal wind stress anomalies (minus the regression against model Niño3) of System-1 (left) and System-2 (middle). These are similar to the SST pattern associated with Niño4 variability apart from the part varying with Niño3 (right).

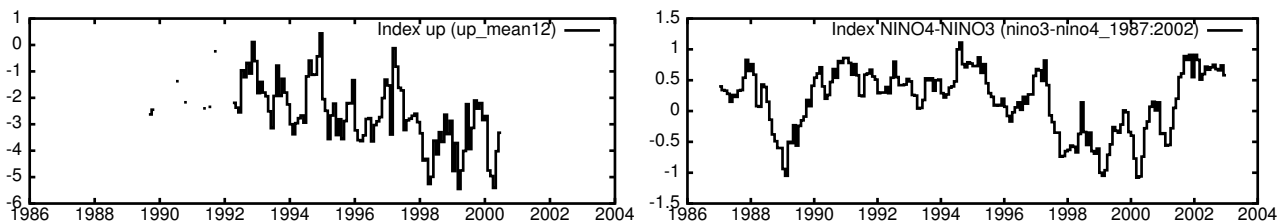


Figure 11: The observed mean zonal wind stress anomalies and Niño4 index (both minus the regression against Niño3).

5 Conclusions

For the ENSO cycle, the MJO as defined by intraseasonal variations in upper-atmosphere indices does not seem to be relevant. In contrast, the influence of surface zonal wind in the equatorial wave guide (5°S – 5°N , 130°E – 160°W) is large, as can be expected from Kelvin wave dynamics and local surface feedbacks. It is partitioned evenly between the linear effects of integrated zonal wind stress and the non-linear effects of the variability of the zonal wind stress, both of which have clear lagged relationships with anomalous evolution of the Niño3 index a few months later ($r \sim 0.5$ for monthly data). The first is easy to understand as the linear integration of a high-frequency signal into a lower-frequency one. The resulting variable is almost equal to the Warm Water Volume and Available Potential Energy used in other analyses. It is also forecast well (r 0.75 for 3-monthly data) by the ECMWF seasonal forecast systems, based on the variability in the central Pacific that is not in phase with the eastern Pacific. The predictability of the variability of zonal wind stress in the equatorial wave guide has not yet been studied here.

References

- Burgers, G. and G. J. van Oldenborgh, 2003: On the impact of local feedbacks in the central Pacific on the ENSO cycle. *J. Climate*, **16**, 2396–2407.
- Fedorov, A. V., S. L. Harper, S. G. Philander, B. Winter, and A. Wittenberg, 2003: How predictable is El Niño? *Bull. Amer. Met. Soc.*, **84**, 911–919.
- Galanti, E. and E. Tziperman, 2000: ENSO's phase locking to the seasonal cycle in the fast-SST, fast-wave, and mixed-mode regimes. *J. Atmos. Sci.*, **57**, 2936–2950.

- Galanti, E. and E. Tziperman, 2002: The equatorial thermocline outcropping — a seasonal control on the tropical Pacific ocean-atmosphere instability strength. *J. Climate*, **15**, 2721–2739.
- Kessler, W. S., 2002: Is ENSO a cycle or a series of events? *Geophys. Res. Lett.*, **29**, 2125–2128.
- Madden, R. A. and P. R. Julian, 1971: Detection of a 40–50 day oscillation in the zonal wind in the tropical Pacific. *J. Atmos. Sci.*, **28**, 702–708.
- McPhaden, M. J., 1999: Genesis and evolution of the 1997-98 El Niño. *Science*, **283**, 950–954.
- McPhaden, M. J., A. J. Busalacchi, R. Cheney, J. R. Donguy, K. S. Gage, D. Halpern, M. Ji, P. Julian, G. Meyers, G. T. Mitchum, P. P. Niiler, J. Picaut, R. W. Reynolds, N. Smith, and K. Takeuchi, 1998: The Tropical Ocean Global Atmosphere (TOGA) observing system: a decade of progress. *J. Geophys. Res.*, **103**, 14169–14240.
- Neelin, J. D., D. S. Battisti, A. C. Hirst, F.-F. Jin, Y. Wakata, T. Yamagata, and S.E. Zebiak, 1998: ENSO theory. *J. Geophys. Res.*, **103**, 14261–14290.
- Reynolds, R. W., N. A. Rayner, T. M. Smith, D. C. Stokes, and W. Wang, 2002: An improved in situ and satellite SST analysis for climate. *J. Climate*, **15**, 1609–1625.
- van Oldenborgh, G. J., 2000: What caused the onset of the 1997–1998 El Niño? *Mon. Wea. Rev.*, **128**, 2601–2607.
- van Oldenborgh, G. J., G. Burgers, S. Venzke, C. Eckert, and R. Giering, 1999: Tracking down the ENSO delayed oscillator with an adjoint OGCM. *Mon. Wea. Rev.*, **127**, 1477–1496.
- Xue, Y., 2003. Daily Madden-Julian Oscillation indices. www.cpc.ncep.noaa.gov/products/precip/CWlink/daily_mjo_index/mjo_index.html.